Silhouette-based 3D Model Reconstruction from Multiple Images

Adem Yaşar Mülayim, Ulaş Yılmaz, Volkan Atalay

Abstract— **The goal of this study is to investigate the reconstruction of 3D graphical models of real objects in a controlled imaging environment and present the work done in our group based on silhouette-based reconstruction. Although many parts of the whole system have been well-known in the literature and in practice, the main contribution of the paper is that it describes a complete, end-to-end system explained in detail. Based on a multi-image calibration method, an algorithm to extract the rotation axis of a turn-table has been developed. Furthermore, this can be extended to estimate robustly the initial bounding volume of the object to be modeled. The disadvantages of the silhouette-based reconstruction can be removed by an algorithm using photoconsistency. This algorithm has a simpler visibility check, and it eliminates the selection of threshold existing in similar algorithms. Besides, in order to construct the appearance, we use the concept of particles. The reconstruction results are shown both on real world and synthetic objects.**

Keywords— **3D object modeling, silhouette-based reconstruction, photoconsistency, texture mapping**

I. INTRODUCTION

RECONSTRUCTION of a complex three dimensional (3D) rigid object from its two dimensional (2D) images is a challenging computer vision problem under general imaging conditions. Without *a priori* information about the imaging environment (camera geometry, lighting conditions, object and background surface properties, etc.), it becomes very difficult to infer the 3D structure of the captured rigid object. For practical 3D reconstruction solutions, the problem can be simplified by using controlled imaging environments. In such an environment, camera makes a controlled motion around the object, and background surface and lighting are selected to reduce the specularities on the acquired image. A setup consisting of a rotary table (turn-table) with a fixed camera is generally used in order to obtain a controlled camera motion around the object [1], [2]. The camera has to be calibrated in such a setup to obtain the internal and external parameters defining the physical properties of the camera and the camera imaging positions with respect to the rotary table turn angles [1], [2], [3], [4], [5] although other alternatives also exist [6]. A silhouette-based volume intersection algorithm can then be applied to reconstruct a coarse 3D volume (approximated visual hull) of the object by using the previously obtained camera parameters for the acquired images [1], [2], [6], [7], [8], [9], [10], [11], [12], [13], [14]. Furthermore, in order to give a realistic appearance to the constructed model, texture or the color information can be added [15], [16], [17], [18], [19], [20], [21].

In this paper, we describe a 3D object modeling system using silhouette-based volume intersection method for reconstruction under a controlled imaging environment and present the work done in our group for such a reconstruction. In order to capture images around an object and to find the camera parameters corresponding to these views, we use an acquisition system composed of a fixed camera and a rotary table as shown in Figure 1.

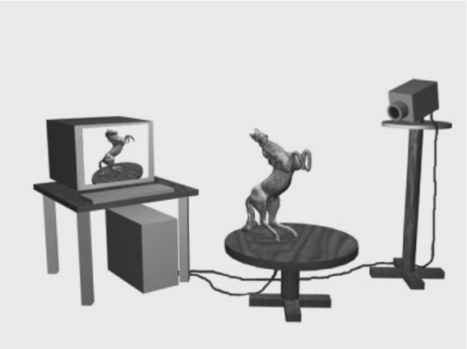

Fig. 1. System setup for image acquisition.

The system diagram is shown in Figure 2, and its details are discussed in the remaining sections of this paper. In order to compute the parameters of the camera, we use a multi-image calibration approach [22]. Due to our acquisition setup, the rotation axis and distance from the camera center to this rotation axis remain the same during the turns of the table. Based on this idea, a vision-based geometrical calibration algorithm have been developed for the rotary table [3]. One of the advantages of this algorithm is that it is more robust than the single image calibration methods. Furthermore, we can compute very easily the distance between the rotation axis of the table with respect to the camera center which in fact facilitates the calculation of the bounding box [23]. The initial estimation of the bounding box is not an essential step but leads to more efficient computations in the subsequent steps. Keeping the number of voxels constant, the size of the bounding box affects the resolution of the final model: smaller the box, less the quantization effects. Use of particles during the appearance reconstruction is a relatively new topic and we have been able to implement this idea although there are also similar studies [19]. There are disadvantages of the silhouette-based reconstruction algorithm. In this context, we have implemented an algorithm which removes the dis-

Ulaş Yılmaz and Volkan Atalay are working at the Department of Computer Engineering, Middle East Technical University, TR-06531, Ankara, Turkey as research assistant and associate proffesor, respectively. Adem Yaşar Mülayim had recently received his PhD from the same Department. Emails: adem@ceng.metu.edu.tr, ulas@ceng.metu.edu.tr and volkan@ceng.metu.edu.tr.

advantages using photoconsistency [24]. Although many parts of the whole system have been well-known in the literature and in practice, the main contribution of the paper is that it describes a complete, end-to-end system explained in detail in which the essential algorithms are given so that interested reader can easily implement the approach.

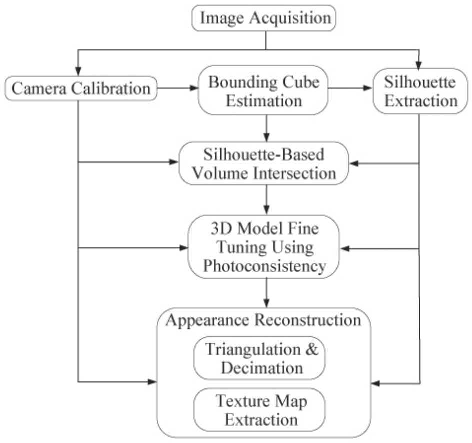
Image Acquisition
Camera Calibration
Bounding Cube Estimation
Silhouette Extraction
Silhouette-Based Volume Intersection
3D Model Fine Tuning Using Photoconsistency
Appearance Reconstruction
Triangulation & Decimation
Texture Map Extraction

Fig. 2. System diagram for silhouette-based method for 3D reconstruction.

The organization of this paper is as follows. We first describe the related studies and the systems in the following section. Vision-based geometrical calibration algorithm, extraction of the rotation axis and a robust estimation of the initial bounding box are explained in Section III. The voxelization of this initial volume with respect to the images is given in IV. Our model fine tuning approach is described in detail in Section V. In Section VI, surface triangulation of the resultant volume and the appearance reconstruction of the triangulated model is explained. Sample reconstructions are shown in Section VII. The paper concludes with Section VIII in which we discuss the presented study and state eventual improvements.

II. RELATED STUDIES AND SYSTEMS

Early passive 3D object model reconstruction attempts have been based on image matching. This class of methods includes multi-view stereo which recovers 3D geometry by using correspondences across images, and by applying surface fitting and triangulation over the estimated 3D clouds of points [10], [25], [26]. The disadvantages of multi-view stereo can be stated as follows. In order to find effective correspondences, views must be close together and correspondences must be found in the images. Resultant partial 3D clouds of points for different views must be triangulated and fused into a single consistent model. In case of sparse correspondence, a parameterized surface model has to be fit to represent the sparse 3D points for surface modeling. Explicit handling of occlusion between views is not addressed.

In order to avoid multi-view stereo drawbacks, model-based multi-view stereo approaches are proposed [27]. Model-based techniques differ from traditional stereo in that they measure how the actual scene of the images deviates from an initially given approximate 3D model. Model-based approach reduces the correspondence problem for views which are relatively apart. Occlusion problem is also addressed by the use of an initial model and fusion of view-based partial surfaces is eliminated. However, model-based multi-view stereo approaches need an initial 3D geometric model which brings additional user interaction.

In order to avoid the disadvantages of multi-view stereo and model-based stereo, 3D scene space solutions are recently proposed [28], [29], [30]. These methods represent the volume of the object by making occupancy decisions about, whether a volume element (voxel) contains object volume in 3D scene, and called as *volumetric scene modeling methods*. Volumetric modeling methods allow views to be captured apart from each other which may cause problems in other methods. More importantly, they eliminate correspondence problem. On the other hand, the final model evolves from an initial volumetric scene representation in which the object of interest lies. In this context, there is no need to fuse an initial model and resultant 3D object data which is the case in multi-view and model-based stereo systems. Occlusion problem is also addressed by using regular tessellation of initial bounding volume as voxels. However, volumetric modeling of object space depends on the calibration of the cameras for each image, and on an initial bounding volume of the object space.

Volumetric scene modeling approaches are basically grouped into two: shape from silhouettes and shape from photoconsistency. Shape from silhouettes techniques deal with the reconstruction of 3D solid models by volume intersection from a set of silhouette images as performed in this study. Silhouette-based 3D reconstruction from a finite image sequence constructs the approximated visual hull of the object. Some excess volume is produced in this approximated visual hull due to the concavities existing on the object and the insufficient camera viewing variety. It is impossible to engrave the additional volume filling the concavities, even if infinite number of images is used in the process. Rather than using binary silhouette images, shape from photoconsistency techniques employ the additional photometric information (color) [28], [29]. This also improves reconstruction results at the excess voxels existing in the approximated visual hull. Shape from photoconsistency methods use the color consistency constraint [28] to distinguish object surface voxels from other voxels. Color constraint for a voxel states that a surface voxel has color consistent projection regions on the images from which it is seen. Use of shape from photoconsistency approach avoids point correspondence difficulties. 3D reconstruction based on photoconsistency requires camera parameters for each used view and a model for the object surface reflectance. Furthermore, a very important issue in these methods is the criterion for consistency check. Most of the consistency criteria require a threshold or an input from the user. In addition, voxel visibility problem has to be well addressed since the color consistency check for a voxel requires the set of images from which the voxel is visible. Efficiency in the visibility test for every voxel is essential. In order to easily maintain visibility information for voxels, voxel coloring algorithm proposed by Seitz and Dyer [28] restricts the position of cameras so that no object point is contained within the convex hull of the camera centers. However, there are several extensions to the initial voxel coloring algorithm for the visibility problem [29], [30], [31], [32], [33]. Instead of using these extensions and alternatives requiring additional space and complex updates as carving progress, or using multi sweeps along the coordinate axes, traversing a ray from the voxel center through the camera center is proposed to check visibility in our study. It is also possible to find the maximum photoconsistent voxels on the ray and this eliminates threshold checks while carving the voxel from the initial set. This algorithm is mostly inspired from Matsumoto et.al. [14].

In the recent years, there was a significant interest in 3D reconstruction from uncalibrated views [6], [34], [35], [36]. These auto-calibration techniques have been the object of a tremendous amount of work [37], [38], [39], [40], [41] and effective methods to derive the epipolar geometry and the trifocal tensor from point correspondences have been devised [6], [42]. However, most of these methods assume that it is possible to run an interest operator such as a corner detector [6], [41] to extract from one of the images a sufficiently large number of points that can then be reliably matched in the other images. When using images exhibiting too little texture, such interest points are not reliable. It has been shown that projective, affine and Euclidean reconstructions can be obtained from uncalibrated views [36], [37], [43], [44], [45]. However, these methods are sensitive to noise and initialization [45] and generally, the reconstruction results are valid up to a scale factor.

Historically, one of the first complete 3D modeling system based on silhouette images is the series of studies by Niem et.al. [1], [46] which is also called Hannover system. Many concepts and techniques of the current systems are based on the ones explained and implemented in this system. In the Hannover system, although there is an attempt to refine the model, the method is not explained demonstrated well. Another system has been proposed by Matsumoto et.al. [2]. Several concepts, such as voting in the implementation of volume intersection are introduced by this group. Furthermore, carving the voxels of the model resulting from shape from silhouette by the use of multiple view-based stereo has also been described [14]. On the other hand, the details and the experimental results are not given. The system described by Gibson et.al. [47] requires no pre-calibration of the camera and uses full perspective geometry. The authors claim that self-calibration is used. However, there is no detailed information given in the paper regarding to this subject. Fitzgibbon et.al. [6] describe the projective geometry of single axis rotation (rotation similar to that discussed in our work) and give its automatic and optimal estimation from an image sequence. However, it is shown that 3D structure and cameras can be calibrated up to an overall two-parameter ambiguity. The two parameter reconstruction ambiguity is removed by specifying camera aspect ratio and parallel scene lines. Apart from the use of uncalibrated multiple views, the system is very similar to that of Hannover. In addition, the work does not indicate any further refinement to remove disadvantages of volume intersection method. A study which is in the same direction as the previous one is by Mendonça et.al. [48] in which a method is described for motion estimation for an object rotating around a fixed axis. Based on this information, 3D positions of the points on the contours of the object is then found by the triangulation and epipolar parameterization. The method is relatively simple and elegant, particularly compared to that proposed by Fitzgibbon et.al. [6] since a few number of correspondences is sufficient. One point which is not very clear in the study of Mendonça et.al. [48] is that for the reconstruction of an object model, some kind of interpolation would be required since only contour information is used. Furthermore, only a few number of results are demonstrated. Our study has several common points with the work by Schmitt et.al. [19], [49]. However, our work differs particularly in the calibration, bounding box finding and the carving aspects.

III. VISION-BASED GEOMETRICAL CALIBRATION OF A TURN-TABLE AND EXTRACTION OF ROTATION AXIS

In a setup consisting of a rotary table with a fixed camera, we use only but at least three images of the calibration pattern to determine the rotation axis position with respect to the fixed camera geometry [3], [4]. Rotation axis can be defined in the fixed camera geometry by calculating the vector u representing the rotation axis itself and the perpendicular distance D between the camera optic center O_c and the rotation axis as seen in Figure 3. In this calibration approach, it is possible to calculate external camera parameters with respect to the initial position and orientation, for any rotation around the rotation axis.

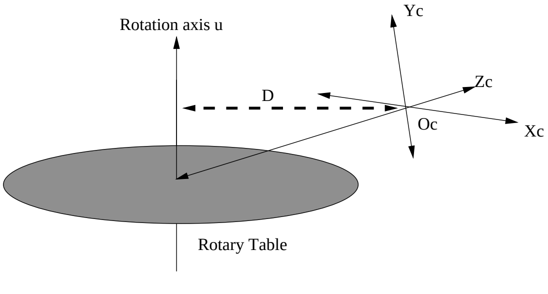

Fig. 3. Rotation axis with respect to camera geometry.

One major source of calibration error is the inaccuracy in the 3D to 2D mappings of the n known points. These can come either from the 3D part (inaccuracy in the fabrication of the geometrical calibration target) or from the 2D part (inaccuracy in the detection of the projected pattern). Lavest et.al. [22] propose a multi-image camera calibration approach to estimate the precise 3D coordinates of the geometrical calibration target when the intrinsic and extrinsic camera parameters represented by unknown vector. This calibration algorithm can be thought to use inherently the concept of bundle adjustment in which 2D image measurements (correspondences) are used to produce jointly optimal 3D structure and viewing parameter estimates. The motivation of Lavest et.al.'s [22] work is that we don't need accurate calibration patterns. However, 3D positions of calibration pattern points provide an initial guess. Then, starting from the 2D positions of pattern points extracted from images, the camera parameters for the image sequence and the 3D positions of pattern points are estimated. Therefore, we may say that Lavest et.al.'s [22] method is a bundle adjustment.

Rotation axis of the turn-table with respect to the fixed camera coordinate frame can be defined by a unit vector u in the direction of the rotation axis and by the translation vector D perpendicular to u, corresponding to the projection of the optical center of the camera onto the rotation axis as shown in Figure 3. Using the rigid transformations Q_i between the fixed camera and position i of the calibration pattern, a vector u representing the rotation axis, and a point p on this vector defined in the camera coordinates can be calculated geometrically [3], [4]. This is totally a geometric computation which does not depend on an estimation procedure. In our study, we use the extracted rotation axis to estimate the initial bounding box of the object in the silhouette-based reconstruction.

If the camera parameters and the object silhouettes on the images are known, the coarse object volume which is in fact a convex hull of the object can be computed. In this procedure, we first estimate the bounding box which is the rectangular prism or box having the minimum volume and at the same time including the object. Since the rotation axis of the rotary table is defined with respect to the camera geometry by the calibration process, the bounding box is calculated easily by backprojecting the silhouette bounding rectangles from all of the imaging views and then intersecting the resultant open volumes [23].

IV. Voxelization

After obtaining the bounding box of the object to be modeled, we then discretize it by dividing into small cubes or voxels. Assuming that each side of the box is divided into n voxels, a voxel space V containing n^3 voxels is generated. Subsequently, we project each cube in the voxel space V onto the images by using the related camera parameters. If the projected cube region on any selected image is totally not contained by the silhouette region, it is removed from the voxel space. Otherwise, it is kept in the object voxel space either as the 'ON' voxel or as the 'IN' voxel with respect to the result of voxel projection region tests for all the views. Algorithm 1 basically gives the idea.

Algorithm 1 Algorithm to compute the voxels of the voxel space which are not out of the object.

```
V_object = {}

FOR ALL voxel v in voxel space V DO
  minVoxelStatusValue = 1.0
  FOR ALL image i = 0..numberOfImages-1 DO
    voxelRegionOnImage = projectVoxelRegionOnImage(v, i)
    voxelStatusValue = regionTest(voxelRegionOnImage, i)
    IF voxelStatusValue < minVoxelStatusValue THEN
      minVoxelStatusValue = voxelStatusValue
    END IF
  END FOR
  IF voxelStatusValue == 0.0 THEN
    voxelStatus = OUT
  ELSE IF voxelStatusValue == 1.0 THEN
    voxelStatus = IN
  ELSE
    voxelStatus = ON
  END IF
END FOR

FOR ALL voxels v in voxel space V DO
  IF voxelStatus != OUT THEN
    V_object = V_object U v
  ENDIF
END FOR
```

V. 3D Model Fine Tuning Using Photoconsistency

Silhouette-based 3D reconstruction using a finite set of object images results in an approximated visual hull of the object. The obtained visual hull is guaranteed to enclose the object in 3D space, since it is the maximal shape which gives the same silhouette as the actual object images for all camera views used in the acquisition of the images. However, excess voxels (volume) is produced in the visual hull which is approximated by a silhouette-based volume intersection approach, because of the concavities on the object and the insufficient camera viewing variety. Since it is very challenging to find the best views to eliminate the excess voxels coming from the insufficient camera viewing variety, and it is impossible to engrave the additional voxels filling the concave regions, silhouette-based reconstruction have to be augmented with another method. Using photometric information existing in the consecutive images from the acquired image sequence is a practical candidate, if the object surface contains well grained texture and if there exists corresponding regions in the consecutive images.

In the practical turn-table and a fixed camera acquisition environment, if the turn angle between each acquisition step is smaller than 180^o, consecutive images from the sequence would contain the same object regions as the object topology permits. The area of this common observation regions for the consecutive camera positions increases as the turn step angle decreases.

In the approximated visual hull of the object obtained from finite set of images, each surface voxel has a set of images from which the voxel can be seen. If it is assumed that a surface voxel placed in correct depth meaning that it is on the real object surface, then stereo theory states that its projections on the images from which it can be seen, must be the corresponding regions. In other words voxels in the approximated visual hull, having correct depth placement have photoconsistent projections on the images from which voxels are seen without occlusion.

The idea, theory and algorithm of using photoconsistency and carving in volumetric voxel spaces is first introduced by [28] and have recently been improved by several researchers [14], [28], [29], [30], [50]. The approaches using photoconsistency is generally called voxel coloring. Starting from an initial set of opaque voxels, voxel coloring algorithm carves the voxels that are not photoconsistent as it iterates on the opaque voxels. The algorithm stops when all the opaque voxels are color consistent. However, in these studies either the approach is not applicable to our case or there is no clear explanation for the implementation. Therefore, here we describe in detail how the previous ideas can be applied to our case and efficiently implemented.

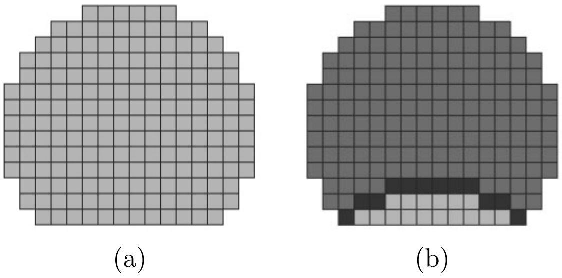
(a) (b)

Fig. 4. (a) 2D cross section of an initial reconstructed volume and (b) real object boundary.

Figure 4 (a) illustrates a 2D cross-section. Each cube in the produced 3D grid of the initial volume is actually a hypothesis for the correct object model, since there exist excess cubes on the generated model related with the drawbacks of the silhouette-based reconstruction. This means that any selected voxel on the generated model can be placed in the object volume, on the object surface or out of the object volume. Figure 4 (b) illustrates real object boundary on its initially reconstructed model which is shown as a 2D slice in Figure 4 (a). In this figure, bolder cubes show the actual border of the object surface at the concavity region. Other cubes are either inside of the object or outside of the object. Initially, we have the hypothesis for every cube that it is on the object surface. This assumption brings a measure, helping in testing the validity of the hypothesis about the cube. Since the cube is assumed to be on the surface, its projections onto the images, from which it can be seen, must be the corresponding regions on different combinations of the image pairs and the texture and color properties of these corresponding cube projections must be nearly the same assuming that the lighting conditions are the same for each view.

In order to test the photoconsistency of an individual voxel, the image set from which the voxel is visible must be determined correctly and efficiently. Visibility checking is the elusive part of the algorithms based on photoconsistency since opaque voxels occlude each other in a complex and constantly changing pattern as carving progress. To simplify visibility check Seitz and Dyer use *ordinal visibility constraint* on the camera locations bringing single pass visibility test for all opaque voxels [28]. However the ordinal visibility constraint has a significant limitation since it requires all camera locations placed at one side of the scene. Solutions for arbitrary camera placement have been proposed by using multiple plane sweeps along the positive and negative directions of each coordinate axes [29], and by using special data structures named as item buffers and layered depth images [30].

Instead of using item buffers or layered depth images requiring additional space and complex updates as carving progress, or using multi sweeps along the coordinate axes, traversing a ray from the voxel center through the camera center is proposed to check visibility in our study. A voxel v is invisible from a view i if there exists other opaque voxels in between v and the camera center i, otherwise the voxel v is visible. Since it is also possible to find the maximum photoconsistent voxels on the ray, it also helps to eliminate threshold checks while carving the voxel from the initial opaque set. Algorithm 2 which is mostly inspired from Matsumoto et.al. [14] outlines our carving solution.

Algorithm 2 Algorithm to compute the p hotoconsistent voxels.

```
FOR ALL voxel v on V_object DO
  v.vote = MAXVOTE
END FOR

FOR ALL image i = 0..numberOfImages-1 DO
  FOR ALL voxel v visible in image i DO
    voxelsOnRay = getVoxelsOnRay(v, c_i)
    maxConsistency = 0
    maxConsistentVoxelIndex = 0
    FOR ALL voxelsOnRay[j], j = 0..numOfVoxelsOnRay DO
      R_1 = projectVoxelOnImage(voxelsOnRay[j], i)
      R_2 = projectVoxelOnImage(voxelsOnRay[j], i-1)
      R_3 = projectVoxelOnImage(voxelsOnRay[j], i+1)
      voxelsOnRay[j].consistency =
          regionTextureSimilarity(R_1, R_2, R_3)
      IF voxelsOnRay[j].consistency > maxConsistency THEN
        maxConsistentVoxelIndex = j
        maxConsistency = voxelsOnRay[j].consistency
      END IF
    END FOR
    FOR ALL voxelsOnRay[j], j = 0..maxConsistentVoxelIndex DO
      voxelsOnRay[j].vote =
          voxelsOnRay[j].vote - (maxConsistentVoxelIndex - j)
    END FOR
  END FOR
END FOR

FOR ALL voxel v in V_object DO
  IF v.vote < voteThreshold THEN
    removeVoxel(v, V_object)
  END IF
END FOR
```

In the algorithm, each voxel in the object voxel space V_{Object}, starts with a high photoconsistency vote value; that is each voxel on the model generated by the silhouette-based reconstruction is assumed to be on the real object surface. Each view i is then processed in the following manner. For each view i, rays from the camera center c_i through the voxels seen from that view i are traversed voxel by voxel. Each voxel on the ray is projected onto the images $i-1$, i, $i+1$ and the voxel's photoconsistency value is calculated using texture similarity measures among the projection regions on the images $i-1$, i, $i+1$. Then, the voxel with maximum photoconsistency value is found and all the voxels existing between this voxel and the camera center c_i loose votes in an increasing order as they become closer to c_i. This process is repeated for all the rays which can be generated from the view i. When the process is performed for all the views, excess voxels caused by the silhouette-based reconstruction loose most of their initial photoconsistency votes.

Voxel coloring algorithms iteratively process surface voxels by checking whether their photoconsistency values are higher or lower than a predefined threshold. However it is not easy to find a color threshold which succeeds well in both the dark and bright parts of a scene if red-green-blue (RGB) color space is used. Additionally inconsistent lighting makes thresholding even more difficult in a fixed light and a turn-table environment. Threshold selection for the removal of a voxel v can be eliminated by looking at the voxel photoconsistency values on the ray starting from the camera center and passing through the voxel v. Voxels on the ray can also be voted according to their distance from the maximum photoconsistent voxel. Voting approach is selected in our study since it converges to final solution faster than iterative processing of surface voxels. In such a voting approach a *voteThreshold* is used. However an adaptive *voteThreshold* value can be selected easier than a predefined photoconsistency threshold. Also it can be selected as a small value in our algorithm to guarantee false voxel removals stay at minimum with the cost of slower convergence.

VI. APPEARANCE RECONSTRUCTION

For the sake of simplicity in texture mapping and visualization of the reconstructed object in 3D, volumetric voxel representation should be transformed to a representation by triangular patches. A simple and practical technique, called as Marching Cubes algorithm [51], [52] is generally used in the computer graphics society to do such a conversion. Marching cubes algorithm uses the isolevel information of the vertices of the voxel in order to interpolate an isosurface passing through the voxel. Having constructed the geometry of the object, we need to recover the appearance; that is the texture of the surface should be determined. Texture mapping is a well-known technique that is used to achieve a high degree of realism in virtual reality applications.

In image-based 3D model reconstruction, the texture of the model is extracted from the images of the object. This increases the realism of the reconstructed model considerably [18]. In spite of its drawbacks due to the lack of the third dimension information, conventional 2D texturing remains the most popular approach in texture mapping. In our system, we use 2D textures, but to reduce the drawbacks of 2D texturing, the concept of particles is used, [19], [53], [54], [55], [56]. We do an abstraction on the actual representation; we consider our model to be a surface composed of 2D particles with three attributes:

1. position, $\overrightarrow{P}(x, y, z)$
2. normal, $\overrightarrow{N}(x, y, z)$
3. color, $\overrightarrow{C}(h, s, v)$.

The position and color information of each particle is embedded in a 2D texture map, and the normal information is stored in the vertices of the triangle on which the particle lies. Each particle's position is computed using a mapping from the texture space to the model space. On the other hand, to assign a normal vector to a particle, the normal vectors of the triangle vertices are used as shown in Figure 5. Bilinear interpolation model which enforces a smooth normal distribution for the particles on the surface enables the extraction of more continuous appearance. A texture element is associated with a particle in a triangle with the following equations:

$$\overrightarrow{P} = (1 - s - t)\overrightarrow{v_0} + (s)\overrightarrow{v_1} + (t)\overrightarrow{v_2} \qquad (1)$$

$$\overrightarrow{N} = (1 - s - t)\overrightarrow{n_0} + (s)\overrightarrow{n_1} + (t)\overrightarrow{n_2} \qquad (2)$$

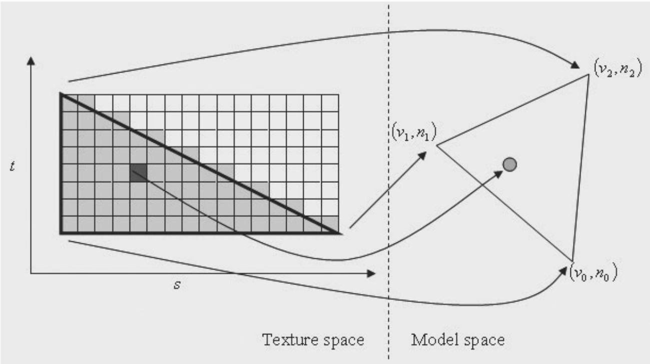

Fig. 5. Association between the texture map and the surface particles of a triangle.

Having assigned a normal and a position to a particle, its color is extracted from the photographs of the object. Each texture element in the texture map corresponds to a surface particle. For each particle, there is a set of source photographs to extract the color. In the histogram of this set, small peaks correspond to inconsistent color entities, while the main peak around which the histogram concentrates is the photoconsistent color of that particle. Having eliminated the inconsistent colors, fusion of the consistent ones can be performed either by merging or by selecting. Merging may distort the high quality textures, thus in our approach, the best candidate is *selected* as described in Algorithm 3.

Algorithm 3 Algorithm to recover the color of a particle.

```
color = DEFAULTCOLOR
C = {}

FOR ALL image i = 0.. numberOfImages-1 DO
  IF particle P is visible in image i THEN
    candidateColor = getColorOfParticleFromImage(P, i)
    candidateColorWeight =
        getDotProductOf(-cameraVector, particleVector)
    C = C U {(candidateColor, candidateColorWeight)}
  END IF
END FOR

histogram = getHistogramOf(C)
C = discardInconsistentColorsFrom(C, histogram)
color = candidateColor with maximum candidateColorWeight
```

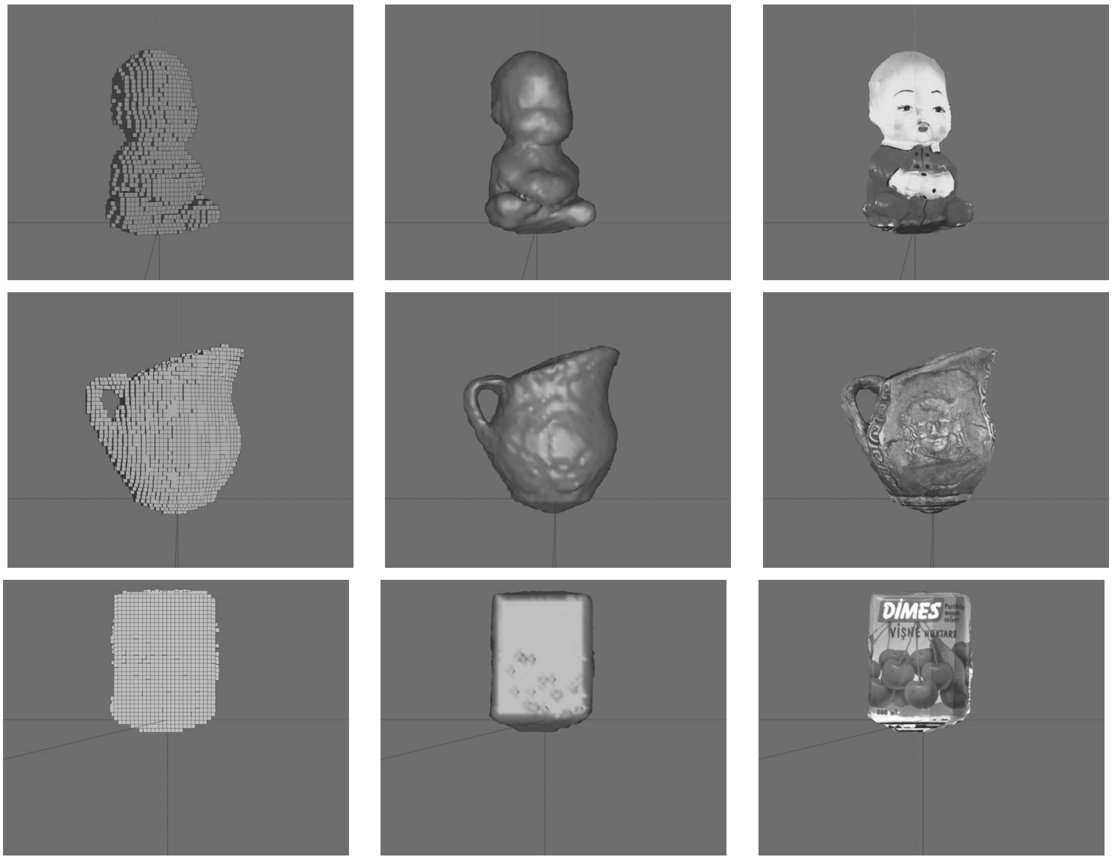

Fig. 6. "toy", "cup" and "box" models after the voxelization, triangulation and appearance reconstruction steps.

VII. Sample Reconstructions

In this section, sample reconstructions output by the described system are demonstrated. First, we give 3 models constructed by the silhouette-based volume intersection method. Then, we show two other models, one constructed from a synthetic image sequence and another one from a real image sequence which are refined by further processing the concave regions using photoconsistency. The images are captured with a digital camera of 1294x1030 pixel size and the longest side of the initial bounding box is divided into 70 voxels. Figure 6 demonstrates "toy", "cup" and "box" models after the voxelization, triangulation and appearance reconstruction steps. "toy" and "cup" sequences are composed 18 images since these objects are more complicated and "box" sequence contains 12 images.

Figure 7 (a), (b), (c) and (d) show the original image, approximated visual hull of the model represented by voxels, refined model using photoconsistency and the triangulated final model, respectively. The image sequence is artificially generated by a renderer. There is a single concave region which is generated to be filled of excess voxels when only silhouette-based volume intersection method is used. It can be explicitly observed that the concave region is successfully modeled.

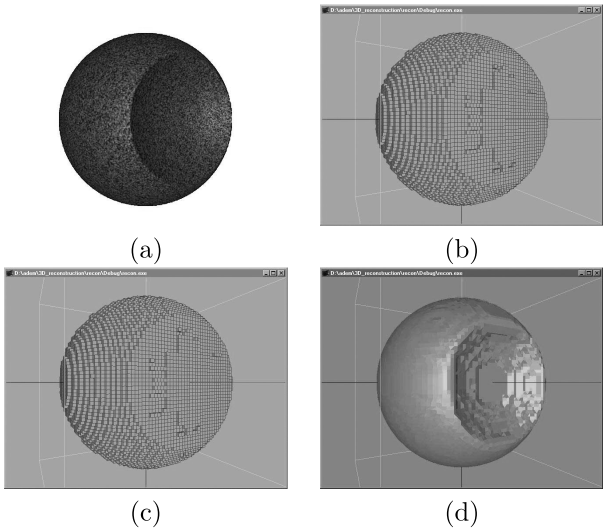

(a) (b) (c) (d)

Fig. 7. (a) Original image, (b) approximated visual hull of the model represented by voxels, (c) refined model using photoconsistency and (d) triangulated final model.

In Figure 8 (a), the original model is manually constructed to have a particular concavity on a box. A simple concavity type is selected since our aim to prove that the algorithm works fine on a real object. Figure 8 (b) and (c) demonstrate silhouette-based volume intersection results represented by polygons and texture, respectively. It can be easily observed that the concave region is filled and therefore, the appearance is also incorrectly constructed in this region. Particularly, the patterns inserted in the concave region are distorted and this can be observed clearly on their slopes. Figure 8 (d) and (e) show refined model by further processing the concave region using photoconsistency. Concave region can then be observed and therefore the patterns mapped on this region have a better appearance.

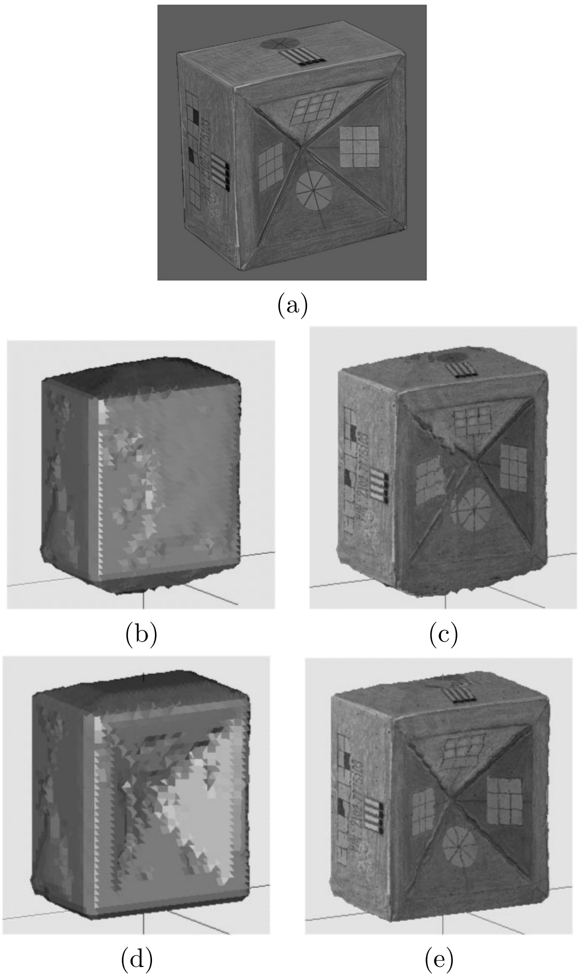

Fig. 8. (a) Original image, (b) silhouette-based volume intersection results represented by polygons and (c) by texture, (d) refined model by further processing the concave region using photoconsistency represented by polygons and (e) by texture.

VIII. CONCLUSIONS AND FUTURE WORK

3D object model reconstruction using silhouette-based volume intersection is a simple and robust method, but it has some drawbacks. In this paper, a complete image-based 3D model reconstruction system is described in detail. Based on a multi-image calibration method, an algorithm to extract rotation axis of a turn-table has been developed. Furthermore, this can be extended to estimate robust and smaller initial bounding volume of the object to be modeled. Better estimation of bounding volume helps in producing better voxel representation of the visual hull of the object. Keeping the number of voxels constant, the size of the bounding box affects the resolution of the final model: smaller the bounding box, lesser the quantization effect on the model.

The main drawback of the silhouette-based volume intersection approach is the additional excess volume coming from insufficient number of viewing positions and from the concavities on the object to be modeled. In order to carve excess voxels from the inferred visual hull which is approximated by silhouette-based volume intersection, an algorithm based on photoconsistency is developed. Voxel visibility checking and photoconsistency threshold in deciding removal of a voxel are the elusive parts of the carving algorithm. Instead of using camera placement constraints or recently developed alternatives requiring additional space and complex updates as carving progress, or using multi sweeps along the coordinate axes, traversing a ray from the voxel center through the camera center is proposed to check visibility in our study. A voxel is visible from a given camera if there is no other opaque voxels in between them. Visibility check starts from a surface voxel and trace the voxel space on the voxel to camera ray. If an opaque voxel is met, then the algorithm stops and decides that the voxel is invisible. Better estimation of initial bounding volume helps again in cutting the visibility search space on a ray since the search is cut at the boundaries of the bounding volume. Recent space carving and voxel coloring approaches use a predefined photoconsistency threshold to decide removal of a voxel from the object voxel space. In these approaches, different results are obtained by using different choices of the photoconsistency threshold. It is not easy to find a color threshold which succeeds well in both the dark and bright parts of a scene if red-green-blue (RGB) color space is used. Also, inconsistent lighting, which is an important problem with a fixed light source and an object rotating on a turn-table, makes thresholding even more difficult. The CIELab color space can be used instead of RGB space to apply a single color threshold for the bright and dim portions of the scene, and using a color space separating chromaticity and luminance may reduce the inconsistent lighting problem, but the problem of a good threshold selection still remains. In our study, threshold selection is eliminated by finding the maximum photoconsistent voxel on the ray starting from the camera center and pass through a selected surface voxel.

Our results show that the excess voxels can be removed successfully. Results of the described algorithm are demonstrated on a synthetic and a real object.

Unlike recent space carving and voxel coloring methods representing the final appearance by giving photoconsistent colors to each voxel, the resultant carved solution is triangulated in our studyö and the final appearance is obtained by using the concept of particles. The surface, in addition to its actual representation, is considered as a collection of surface particles. The color of each particle is extracted from the images and combined in a 2D texture map. Since particles are smaller primitives, the appearance is continuous on the surface. This is a solution to the boundary discontinuity problem of most previous studies. The employed photoconsistency reduces also the artifacts of bad illumination. Representation of the final model by triangles enables the model to be converted into well known graphical formats such as VRML very easily.

One of the most important progresses to be added to this study is the detection of possible concave regions. Such a detection of concave regions would lower the computational complexity and also avoids the application of the algorithm onto non-concave parts of the model. It can also be interesting to develop an intelligent sculpting tool for the elimination of concave regions.

ACKNOWLEDGEMENTS

This study is partially supported by TÜBİTAK (Scientific and Technical Research Council of Turkey) under the grant EEEAG-199E024, by METU Graduate School of Natural and Applied Sciences and by METU Research Grant. Adem Y. Mülayim's study is supported by TÜBİTAK Integrated PhD Program.

References

[1] W. Niem and J. Wingbermühle, "Automatic reconstruction of 3d objects using a mobile monoscopic camera," in *International Conference on Recent Advances in 3D Imaging and Modeling*, May 1997, pp. 173–180.

[2] Y. Matsumoto, H. Terasaki, K. Sugimoto, and T. Arakawa, "A portable three-dimensional digitizer," in *International Conference on Recent Advances in 3D Digital Imaging and Modeling*, May 1997, pp. 197–204.

[3] A. Y. Mülayim, Y. Yemez, F. Schmitt, and V. Atalay, "Rotation axis extraction of a turn table viewed by a fixed camera," in *Vision Modeling and Visualisation*, November 1999, pp. 35–42.

[4] A. Y. Mülayim, F. Schmitt, and V. Atalay, "Vision-based geometrical calibration of a turn-table for 3d object reconstruction," Tech. Rep. TR-2000-01, Middle East Technical University, 2000.

[5] P. Ramanathan, E. Steinbach, and B. Girod, "Silhouette-based multiple-view camera calibration," in *Vision, Modeling and Visualization*, 2000, pp. 3–10.

[6] A. W. Fitzgibbon, G. Cross, and A. Zisserman, "Automatic 3d model construction for turn-table sequences," in *SMILE Workshop on Structure from Multiple Images in Large Scale Environments*, R. Koch and L. Van Gool, Eds. June 1998, pp. 154–170, Springer-Verlag, http://www.robots.ox.ac.uk/ vgg.

[7] M. Potmesil, "Generating octree models of 3d objects from their silhouettes in a sequence of images," *Computer Vision Graphics and Image Processing*, vol. 40, no. 1, pp. 1–29, October 1987.

[8] R. Szelisky, "Rapid octree construction from image sequences," *Computer Vision Graphics and Image Processing*, vol. 58, no. 1, pp. 23–32, July 1993.

[9] C. S. Zhao and R. Mohr, "Relative 3d regularized b-spline surface reconstruction through image sequences," in *European Conference on Computer Vision*, May 1994, pp. 417–426.

[10] J. Y. Zheng, "Acquiring 3-d models from a sequence of contours," *IEEE Transations on Pattern Analysis and Machine Intelligence*, vol. 16, no. 2, pp. 163–178, February 1994.

[11] W. B. Seales and O. D. Faugeras, "Building 3 dimensional object models from image sequences," *Computer Vision and Image Understanding*, vol. 61, no. 3, pp. 308–324, May 1995.

[12] E. Boyer, "Object models from contour sequences," in *European Conference on Computer Vision*, 1996, pp. 109–118.

[13] S. Sullivan and J. Ponce, "Automatic model construction, pose estimation, and object recognition from photographs using triangular splines," *IEEE Transactions on Pattern Analysis and Machine Intelligence*, vol. 20, no. 10, October 1998.

[14] Y. Matsumoto, K. Fujimura, and T. Kitamura, "Shape-from-silhouette/stereo and its application to 3-d digitizer," in *Discrete Geometry for Computer Imagery Conference, Lecture Notes in Computer Science 1568*, 1999, pp. 177–188.

[15] W. Niem and H. Broszio, "Mapping texture from multiple camera views onto 3d object models for computer animation," in *International Workshop on Stereoscopic and Three Dimensional Imaging*, September 1995, pp. 99–105.

[16] S. Genç and V. Atalay, "Texture extraction from photographs and rendering with dynamic texture mapping," in *10th International Conference on Image Analysis and Processing*, September 1999.

[17] H. P. A. Lensch, W. Heidrich, and H-P. Seidel, "Automated texture registration and stitching for real world models," in *Pacific Graphics*, October 2000, pp. 317–337.

[18] F. M. Weinhaus and V. Devarajan, "Texture mapping 3d models of real-world scenes," *ACM Computing Surveys*, vol. 29, no. 4, pp. 325–365, December 1997.

[19] F. Schmitt and Y. Yemez, "3d color object reconstruction from 2d image sequences," in *International Conference on Image Processing*, October 1999, pp. 65–69.

[20] E. Ofek, E. Shilat, A. Rappoport, and M. Werman, "Multiresolution textures from image sequences," *IEEE Computer Graphics and Applications*, vol. 17, no. 2, pp. 18–29, March-April 1997.

[21] J. P. Neugebauer and K. Klein, "Texturing of 3d models of real world objects from multiple unregistered photographic views," *Computer Graphics Forum*, vol. 18, no. 3, pp. 245–256, September 1999.

[22] J. M. Lavest, M. Viala, and M. Dhome, "Do we really need an accurate calibration pattern to achieve a reliable camera calibration?," in *European Conference on Computer Vision*, 1998, pp. 158–174.

[23] A. Y. Mülayim, O. Özün, V. Atalay, and F. Schmitt, "On the silhouette based 3d reconstruction and initial bounding cube estimation," in *Vision Modeling and Visualisation*, November 2000, pp. 11–18.

[24] A. Y. Mülayim and V. Atalay, "Multibaseline stereo coreection for silhouette-based 3d model reconstruction from multiple images," in *SPIE, Three-Dimensional Image Capture and Applications IV*, January 2001, pp. 24–25.

[25] T. Kanade, M. Okutomi, and T. Nakahara, "A multiple-baseline method," in *DARPA Image Understanding Workshop*, 1992, pp. 409–426.

[26] T. Kanade, S. B. Kang, J. Webb, and C. L. Zitnick, "A multibaseline stereo system with active illumination and real-time image acquisition," in *International Conference on Computer Vision*, 1995, pp. 88–93.

[27] P. E. Debevec, C. J. Taylor, and J. Malik, "Modeling and rendering architecture from photographs: A hybrid geometry and image-based approach," in *SIGGRAPH'96, Computer Graphics Proceedings, Annual Conference Series*, August 1996, pp. 11–20.

[28] S. M. Seitz and C. R. Dyer, "Photorealistic scene reconstruction by voxel coloring," *International Journal of Computer Vision*, vol. 35, no. 2, pp. 151–173, 1999.

[29] K. N. Kutulakos and S. M. Seitz, "A theory of shape by space carving," *Internation Journal of Computer Vision*, vol. 38, no. 3, pp. 1999–218, 2000.

[30] W. B. Culbertson, T. Malzbender, and G. Slabaugh, "Generalized voxel coloring," in *International Conference on Computer Vision*, September 1999, pp. 100–115.

[31] N. Max, "Hierarchical rendering of trees from precomputed multi-layer z-buffers," in *Eurographics Rendering Workshop*, 1996, pp. 165–174.

[32] J. Shade, S. Gortler, L. He, and R. Szelisky, "Layered depth images," in *SIGGRAPH*, 1998, pp. 231–242.

[33] P. Eisert, E. Steinbach, and B. Girod, "Multi-hypothesis, volumetric reconstruction of 3-d objects from multiple calibrated camera views," in *International Conference on Acoustics Speech and Signal Processing*. March 1999, pp. 3509–3512, Phoenix.

[34] M. Pollefeys, R. Koch, M. Vergauwen, and L. Van Gool, "Automated reconstruction of 3d scenes from sequences of images," *Isprs Journal Of Photogrammetry And Remote Sensing*, vol. 55, no. 4, pp. 251–267, 2000.

[35] P. A. Beardsley, P. H. S. Torr, and A. Zisserman, "3d model acquisition from extended image sequence," in *European Conference on Computer Vision*, 1996, pp. 683–695.

[36] R. Koch, M. Pollefeys, and L. Van Gool, "Multi viewpoint stereo from uncalibrated video sequences," in *European Conference on Computer Vision*, 1998, pp. 55–71.

[37] O. D. Faugeras, "What can be seen in three dimensions with an uncalibrated stereo rig?," in *European Conference on Computer Vision*, G. Sandini, Ed., Santa Margherita Ligure, Italy, May 1992, pp. 563–578, Springer-Verlag, Lecture Notes in Computer Science.

[38] R. I. Hartley, "Estimation of relative camera positions for uncalibrated cameras," in *European Conference on Computer Vision*. May 1992, pp. 579–587, Springer-Verlag.

[39] Q. T. Luong and T. Viéville, "Canonical representations for the geometries of multiple projective views," *Computer Vision and Image Understanding*, vol. 64, no. 2, pp. 193–229, 1996.

[40] B. Triggs, "Linear projective reconstruction from matching tensors," *Image and Vision Computing*, vol. 15, no. 8, pp. 617–625, 1997.

[41] M. Pollefeys, R. Koch, and L. Van Gool, "Self-calibration and metric reconstruction in spite of varying and unknown internal camera parameters," *International Journal of Computer Vision*, vol. 32, no. 1, pp. 7–25, 1999.

[42] Z. Zhang, R. Deriche, O. Faugeras, and Q. T. Luong, "A robust technique for matching two uncalibrated images through the recovery of the unknown epipolar geometry," *Artificial Intelligence Journal*, vol. 78, pp. 87–119, October 1995.

[43] R. I. Hartley and A. Zisserman, *Multiple View Geometry in Computer Vision*, Cambridge University Press, September 2000.

[44] S. J. Maybank and O. D. Faugeras, "A theory of self-calibration of a moving camera," *International Journal of Computer Vision*, vol. 8, no. 2, pp. 123–151, 1992.

[45] A. Fusiello, "Uncalibrated euclidean reconstruction: a review," *Image and Vision Computing*, vol. 18, no. 67, pp. 555–563, May 2000.

[46] W. Niem and R. Buschmann, "Automatic modelling of 3d natural objects from multiple views," 1994.

[47] D. P. Gibson, N. W. Campbell, and B. T. Thomas, "The generation of 3d models without camera calibration," in *Computers and Graphics*. June 1998, pp. 146–149, ACTA Press.

[48] P. R. S. Mendonça, K-Y. K. Wong, and R. Cipolla, "Camera pose estimation and reconstruction from image profiles under circular motion," in *European Conference on Computer Vision*, David Vernon, Ed., Dublin, Ireland, June/July 2000, pp. 864–877, Springer-Verlag.

[49] C. H. Esteban and F. Schmitt, "Multi-stereo 3d object reconstruction," in *International Symposium on 3D Data Processing Visualization and Transmission*, G. M. Cortelazzo and C. Guerra, Eds., Padova, Italy, June 2002, pp. 159–166, IEEE Computer Society.

[50] L. Zhang and S. M. Seitz, "Image-based multiresolution modeling by surface deformation," Tech. Rep. CMU-RI-TR-00-07, Robotics Institute Carnegie Mellon University, 2000.

[51] W. E. Lorensen and H. E. Cline, "Marching cubes: A high resolution 3d surface reconstruction algorithm," *ACM Computer Graphics*, vol. 21, no. 4, pp. 163–169, 1987.

[52] C. Montani, R. Scateni, and R. Scopigno, "Discretized marching cubes," in *Visualization*, 1994, pp. 281–287.

[53] W. T. Reeves, "Particle systems - a technique for modeling a class of fuzzy objects," *ACM Transactions of Graphics*, vol. 2, no. 2, pp. 91–108, April 1983.

[54] R. Szelisky and D. Tonnesen, "Surface modeling with oriented particles," *Computer Graphics (SIGGRAPH'92)*, vol. 26, no. 2, pp. 185–194, July 1992.

[55] T. Nishita and Y. Dobashi, "Modeling and rendering of various natural phenomena consisting of particles," in *Computer Graphics International Conference*, July 2001, pp. 149–156.

[56] J. M. Dischler and D. Ghazanfarpour, "A survey of 3d texturing," *Computers and Graphics*, vol. 25, no. 1, pp. 135–151, February 2001.

Adem Yaşar Mülayim has received his PhD in November 2002 from the Department of Computer Engineering at Middle East Technical University, Ankara, Turkey. He also received his BSc and MSc degrees in computer engineering from the same department in 1993 and 1996, respectively. His research interests include computer vision, modeling, terrain image analysis, perceptual organization, image processing and pattern recognition.

Ulaş Yılmaz is a doctoral candidate and a research assistant at the Department of Computer Engineering at Middle East Technical University, Ankara, Turkey. He received his BSc and MSc degrees in computer engineering from Middle East Technical University in 1999 and 2002, respectively. His research interests include computer vision, computer graphics and pattern recognition. He is a member of the Turkish Pattern Recognition and Image Analysis Society.

Volkan Atalay is an associate professor of computer engineering at the Middle East Technical University. Previously, he was a visiting scholar at the New Jersey Institute of Technology. He received a BSc and an MSc in electrical engineering from Middle East Technical University and a Ph.D. in computer science from the Université René Descartes-Paris V, Paris, France. His research interests include computer vision, document analysis and applications of neural networks. He is a member of the IEEE Computer Society and the Turkish Pattern Recognition and Image Analysis Society.